

Gravity effects on first-sound velocity near $T_\lambda(P)$ in liquid ^4He

Félix Vidal and Jesús Maza

*Laboratorio de Física de Materiales, Facultad de Física,
Universidad de Santiago de Compostela, Spain*

(Received 21 May 1986)

Near T_λ , the first-sound velocity is mainly affected by two rounding mechanisms: one, intrinsic, is due to critical dispersion; the other, nonintrinsic, is due to the spatial inhomogeneity induced by gravity in a sample of finite height. Here a detailed analysis of the local and nonlocal gravity effects is made, and a numerical procedure to calculate quantitatively the gravity rounding contribution in the presence of dispersion is proposed. This method is used to separate for what we believe to be the first time gravity and dispersion effects in real measurements. In particular, contrary to a widely held assumption, it turns out that gravity effects appreciably the absolute value of the measured velocity only in the very-low-frequency range (a few kHz or less), independently of the sample height and of how close the system is to $T_\lambda(P)$. It is also shown that the other main gravity effect, the temperature shift of the velocity minimum, is also strongly affected by dispersion. The present numerical procedure permits gravity corrections to (first-) sound velocity in real measurements to be made in a self-consistent way, with high accuracy.

I. INTRODUCTION

The presence of a gravitational field causes the pressure in a fluid to vary with height. As a consequence, each pressure-dependent parameter of the fluid is subject to a gradient. This is the case, for instance, for density, which is coupled to pressure through the compressibility of the system. In general, the coupling coefficients remain finite, and in a sample of reasonable depth (a few cm or less) the corresponding gradients are negligible. However, in the presence of critical phenomena or near phase transitions, the coupling coefficients may suffer very sharp variations or even critical divergences. In such cases the spatial inhomogeneity associated with the gravitational field may be very important.¹ For instance, as is well known, the compressibility of a pure fluid diverges as the fluid approaches the gas-liquid critical point. The gravitational effects on density cannot, therefore, be ignored in the analyses of experiments performed close to this transition.^{1,2}

Although conceptually similar to critical points in pure fluids, the influence of gravity near the λ transition in liquid helium (^4He) arises in a somewhat different and more subtle way. This is mainly due to the fact that the normal-superfluid transition is a critical line instead of a critical point. In addition, this transition does not belong to the same universality class as the usual critical points in fluids.³ The critical behaviors and the corresponding critical exponents of the various parameters which characterize the two transitions are consequently different. This situation is particularly well illustrated by the (first-) sound velocity, u , which may be expressed as a function of both the pressure P and the reduced temperature $t \equiv T - T_\lambda(P)$ where T_λ is the critical temperature (see Fig. 1). In a gravitational field the dependence of u on the height h along the sample may be written

$$\frac{du(h)}{dh} = \left[\frac{\partial u}{\partial P} \right]_t \frac{dP}{dh} + \left[\frac{\partial u}{\partial t} \right]_P \frac{dt}{dh} \\ = \rho g \left[\left[\frac{\partial u}{\partial P} \right]_t - T'_\lambda \left[\frac{\partial u}{\partial t} \right]_P \right], \quad (1)$$

where ρ is the liquid- ^4He density, g is the gravity acceleration, and we have also used $dP/dh = \rho(h)g$, and $T'_\lambda \equiv (\partial T/\partial P)_\lambda$. The first term in Eq. (1) is mainly associated with the isothermal compressibility κ_T of the medium. In contrast with critical points, κ_T diverges weakly near T_λ , so the influence of this term must be weak in

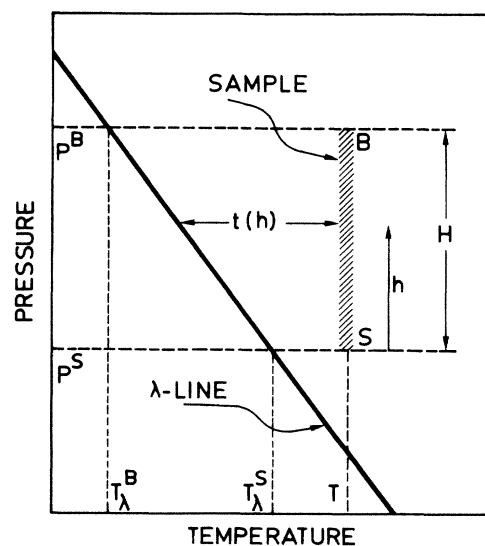


FIG. 1. Schematic diagram of a typical sample at a temperature close to $T_\lambda(P)$.

this transition. The second term is associated with the h dependence of the distance in temperature from the λ line (Fig. 1). This last term, which will be the dominant one near T_λ , does not exist for critical points, for which T_c is obviously independent of h .

Both terms in Eq. (1) act as a nonintrinsic "rounding" mechanism, analogous to those arising from the presence of impurities, finite-sample effects, or nonequilibrium behavior. Such a mechanism originates two main observable effects on the first-sound velocity: a displacement of T_{\min} , the temperature at which the velocity is minimum [for a sample of zero height and in the zero-frequency limit T_{\min} coincides with $T_\lambda(P)$], and a rounding of this minimum and, therefore, an increase of the absolute values of $u(t)$ around T_{\min} . Both effects are relatively small and occur very close to $T_\lambda(P)$. Measurements of first sound precise enough and close enough to T_λ to allow the observation of these effects were first obtained in 1968 by Barmatz and Rudnick.⁴ These data were analyzed in terms of gravity influence by Ahlers,^{5,6} one of whose basic starting points was the adoption, as local velocity, of the functional form suggested by thermodynamics, i.e., the zero-frequency velocity. This approximation, used since then also by other authors,^{7,8} allows straightforward calculations of the spatial averages of the velocity. However, inspection of Eq. (1) shows that its use is not valid when there is dispersion of the velocity (an intrinsic rounding mechanism), especially if quantitative results must be obtained: dispersion changes the dependence of u on P and t near T_λ (drastically in the case of t) and hence also the corresponding coefficients in Eq. (1). It will be seen below that this is so, even at the lower frequencies measured.

The central problem created by the presence of the gravity field, which has been eluded until now, is thus, precisely, the separation of the two rounding mechanisms: one intrinsic, associated with (critical or noncritical) dispersion, and the other, nonintrinsic, due to the spatial gradients induced by gravity, an external field. In this paper, we report on a systematic analysis of the gravity effects on first-sound measurements near T_λ , and a simple and compelling numerical method to separate gravitational and dispersion effects is presented. In addition to its formal interest, an adequate approach of the influence of gravity is crucial for a quantitative comparison between experiments and recent dynamic scaling results on the first sound.⁹ Until now, such a comparison has been restricted to the high-frequency range ($\omega/2\pi \geq 1$ MHz) where, due precisely to the strong critical dispersion, gravity effects have been supposed to be almost suppressed.¹⁰ The validity of this assumption will be proved here. The quantitative confrontation between the very precise first-sound (attenuation and dispersion) data already available and, on the other side, the existing theoretical results with no adjustable parameters,⁹ is playing a central role in some of the most important problems and controversies still open in critical dynamics near T_λ .^{11,12} Furthermore, among some of the more practical motivations of our study, we may invoke two: microgravity experiments,¹³ and the use of low-frequency first sound as a microdegree thermometer near T_λ .¹⁴ This last capability is associated

with the important values of $(du/dT)_P$ in this region. The knowledge of the influence of gravity on this coefficient will also be crucial for this application.

In Sec. II we present a discussion of the different approximations we need to calculate quantitatively the gravity effects. In Sec. III we summarize the calculations of the average thermodynamic (zero-frequency) velocity. Section IV describes the numerical procedure used to separate gravity and dispersion effects in real (nonzero frequency) measurements. Finally, the main conclusions are contained in Sec. V.

II. FRAMEWORK AND APPROXIMATIONS

A. Local and nonlocal gravity effects

A basic starting point of our approach is the hypothesis that the local properties of the fluid can be identified with those of an homogeneous system, i.e., we neglect all possible nonlocal effects due to the gravity field and arising in either the first or the second term in Eq. (1). This implies that the thermodynamic functions vary only because of their dependence on h , but locally they will keep their standard functional form. In other words, we will take into account only the *local* or *implicit* effects associated with the homogeneity breaking produced by gravity, but we are going to neglect the so-called *nonlocal* or *explicit* effects, which would change the functional form of the thermodynamic magnitudes even at the local level.

A direct analysis of this approximation, like that proposed recently for the gas-liquid critical-point transition and based on the so-called squared-gradient theory,¹⁵ requires an equation of state. Unfortunately, such an equation valid around T_λ is not available as yet for ⁴He liquid. However, it is possible to define, in analogy with what has already been done for the gas-liquid critical point,^{1,2} various phenomenological criteria. They are mainly based on two types of qualitative considerations: the apparition of new lengths associated with the gradients induced by gravity as, for example, $\rho(\partial\rho/\partial h)^{-1}$ or $T(\partial t/\partial h)^{-1}$. The breakdown of the local homogeneity will occur when one of these new lengths becomes comparable with some intrinsic characteristic length of the system as, for example, the correlation length of the order parameter or a spatial dimension of the sample or, in our case, the sound wavelength. The second type of phenomenological criterion for the appearance of nonlocal effects is based on the modifications induced by the external gravity field in the spectrum of the spontaneous thermal fluctuations of the system.^{1,15} For example, the sample may become locally inhomogeneous when the potential energy of a fluctuation becomes comparable with its activation energy, $k_B T$, where k_B is the Boltzmann constant.

Let us examine quantitatively some of these criteria in the case of the λ transition of liquid helium. We may begin with those concerning the most relevant characteristic length of the medium, namely, the correlation length ξ of the order parameter. This is because any inhomogeneity affecting the order-parameter behavior will not only modify the functional form of the local fluid properties but will even change the nature of the transition. A first

TABLE I. Some of the characteristic lengths arising in a liquid-helium sample near $T_\lambda(P)$ submitted to the standard gravity field ($g=9.8 \text{ m/s}^2$) and at saturated vapor pressure and $T - T_\lambda^S = 10^{-6} \text{ K}$.

Characteristic length	Correlation length of the order parameter ξ_+	Correlation difference length λ_ξ	Density gradient length λ_ρ	Reduced temperature gradient length λ_T or λ_t	First-sound wavelength at 1 MHz, λ	Typical sample height H
Value at $t=10^{-6} \text{ K}$ and SVP (cm)	2.4×10^{-4}	5×10^{-8}	4×10^5	$\lambda_T = 1.7 \times 10^6$ $\lambda_t = 0.8$	2.2×10^{-2}	0.5–4.5

condition for the onset of nonlocal effects may concern directly ξ : the breakdown of the local homogeneity can be expected when $\xi(t(h))$ starts to vary appreciably, due to the gravity-induced inhomogeneity, over its own length. We may express it as¹

$$\Delta\lambda_\xi = |\xi(t) - \xi(t + \Delta t(\xi))| \gtrsim 10^{-1}\xi(t), \quad (2)$$

where $\Delta t(\xi) = -(\partial T/\partial P)_\lambda \rho g \xi$ is the shift in reduced temperature corresponding to a vertical displacement of extent ξ in the sample. Using

$$\xi(t) = \xi_0 |t/T_\lambda|^{-2/3}, \quad (3)$$

with¹⁶ $\xi_0 = \xi_+ = 1.4 \times 10^{-8} \text{ cm}$ (independent of pressure) and the data of Ref. 17 for the thermodynamic parameters, Eq. (2) leads to the absence of nonlocal effects for $t \gtrsim 10^{-8} \text{ K}$ (see also Table I). Using the numerical information of Ref. 17, we found also that other possible conditions for the applicability of the local homogeneity, as, for instance,

$$\lambda_\rho \equiv \rho \left[\frac{\partial \rho}{\partial h} \right]^{-1} = \frac{1}{\rho g K_T} \gg \xi(t) \quad (4)$$

and

$$\lambda_T \equiv T \left[\frac{\partial t}{\partial h} \right]^{-1} = \frac{-T}{\rho g T'_\lambda} \gg \xi(t) \quad (5)$$

are violated (we work out the limiting conditions $\lambda_{\rho,T}/\xi = 1$) at saturated vapor pressure (SVP) for, respectively, $t \approx 10^{-20} \text{ K}$ and $t \approx 10^{-21} \text{ K}$. Note here that a different length associated with the variations of the distance in temperature to $T_\lambda(P)$ may be obtained by using in Eq. (5) t instead of T . This leads to

$$\lambda_t \equiv t \left[\frac{\partial t}{\partial h} \right]^{-1} \gg \xi(t), \quad (6)$$

and under the same conditions as indicated before, $\lambda_t \approx \xi(t)$ for $t \approx 8 \times 10^{-9} \text{ K}$. However, for all three conditions the breakdown of the local homogeneity will appear for distances in temperature to $T_\lambda(P)$ much smaller than are usually used in experiments ($|t| \gtrsim 10^{-6} \text{ K}$).

Finally, let us check an alternative type of criterion mentioned before and associated with the modifications induced by gravity in the spectrum of the spontaneous thermal fluctuations in the system. For instance, in analogy with what has been proposed by Sengers and co-workers for the gas-liquid critical-point transition,^{1,15} we may compare the gravitational potential energy of a fluctuation of the density number N with its thermal energy

$k_B T$. The mean-square fluctuation of the number of molecules N in a volume V is given by¹⁸

$$(\overline{\Delta N})^2 = \frac{k_B T V \rho^2 K_T}{m^2},$$

where m is the ⁴He atomic mass. Thus, the gravitational potential energy of a spontaneous fluctuation with a volume of the order of ξ^3 is

$$E_P = mg \xi [(\overline{\Delta N})^2]^{1/2} = \rho g (K_B K_T T)^{1/2} \xi^{5/2},$$

and we may expect nonlocal effects to be absent provided that E_P is much less than $k_B T$. The limiting condition $E_P \approx k_B T$ is verified for $|t| \approx 7 \times 10^{-12} \text{ K}$.

In Table I we present an estimate of some of the characteristic lengths arising in a sample subject to the Earth's gravity ($g=9.8 \text{ m/s}^2$) and for $t=10^{-6} \text{ K}$ and SVP. This reduced temperature was chosen because it is the smaller temperature distance to T_λ in typical first-sound experiments.^{7,8,10} The main conclusion from this table is that for attainable temperature intervals there seems not to exist crossover of the different (gravity-independent or -dependent) characteristic lengths to cause the appearance of nonlocal effects.

B. First-sound P dependence versus t dependence

In this paragraph we verify that near $T_\lambda(P)$ the t dependence of first-sound velocity is much stronger than its P dependence. This fact will allow us to greatly simplify our subsequent calculations. In fact, we want to show that in Eq. (1) one has

$$\left[\frac{\partial u}{\partial P} \right]_t \ll -T'_\lambda \left[\frac{\partial u}{\partial t} \right]_P. \quad (7)$$

We analyze this inequality for brevity only at $t \approx 0$ since this is the more significant temperature for gravity effects. As to the P dependence, inspection of first-sound measurements^{8,17} shows that the derivative $(\partial u/\partial P)_t$ is maximum at SVP and of the order of 10^3 cm/s bar . On the other hand, the t derivative is a strong function of frequency. Thus, using the data of Ref. 7, for instance, we obtain at SVP $(\partial u/\partial t)_P \approx 5 \text{ cm/s } \mu\text{K}$ at $\omega/2\pi = 5.4 \text{ kHz}$ and $1 \text{ cm/s } \mu\text{K}$ at 54 kHz . A value of $T'_\lambda = -8.88 \times 10^{-3} \text{ K/bar}$ yields for $-T'_\lambda (\partial u/\partial t)_P$, $4.4 \times 10^4 \text{ cm/s bar}$ and $9 \times 10^3 \text{ cm/s bar}$ at a frequency of 5.4 and 54 kHz , respectively, both values again at SVP and $t \approx 0$. In conclusion, up to some tens of kHz, the right-hand side of Eq. (7) is at least approximately ten times larger than the left-hand side. Besides, it is in this

range of frequency where, as we shall see in Sec. IV, gravity effects are yet appreciable.

Although first sound is not the critical mode of the normal-superfluid transition in liquid ^4He (the critical mode is the thermal one), the privileged role of t may be seen as a consequence of the fact that in this transition the thermodynamic variable directly coupled with the order parameter is temperature, pressure acting as a noncritical (inert) variable. This situation again contrasts with what occurs near the gas-liquid critical point, where the order parameter is precisely the difference between the densities of the gaseous and liquid phases.

C. Measured, local, and average velocities

The measured velocity of first sound propagating along the vertical direction in a sample of depth H will be an average of the local velocity $u_p(t(h), \omega)$. The kind of average depends, in principle, on the experimental procedure used. In the audio and the ultrasonic frequency ranges ($\omega/2\pi \leq 100$ MHz), there are, basically, two such techniques: the pulse propagation and the acoustic resonance in a cavity. Let us write formally the expressions for the averages to be used in both cases. In the first technique, the measured parameter is the (average) flytime T of the pulse throughout the known distance H . In this case, the average velocity can be defined as $\langle u \rangle_{\text{FT}} \equiv H/T$. In this expression, T may easily be related to the local velocity $u(h) = dh/dt$ (here t is the time) to obtain

$$\langle u \rangle_{\text{FT}} = \left[\frac{1}{H} \int_0^H \frac{dh}{u(h)} \right]^{-1}.$$

In the second method, the sound velocities are found by measuring the resonant frequencies (RF), usually of plane-wave modes, in cylindrical cavities. For uniform systems and with such a simple geometry, there exists a straightforward relation between the velocity $u (= \langle u \rangle)$, in this case) and the eigenfrequencies, i.e., ω_{pmn}^2/u^2

$= (\pi\alpha_{mn}/d)^2 + (\pi p/H)^2$, where p , m , and n are “quantum” numbers labeling the mode, d is the cavity radius, and α_{mn} are numbers of order unity. This same relation is used in the case of nonuniform media to define the average measured velocity $\langle u \rangle_{\text{RF}}$ for a given mode. In order to relate $\langle u \rangle_{\text{RF}}$ to the local velocity $u(h)$, we follow the approach proposed by Hohenberg and Barmatz in their analysis of the gas-liquid critical point.² In fact, when $u(h)$ does not vary appreciably between the top and the bottom of the sample, which is our case, application of perturbation theory leads to

$$\langle u \rangle_{\text{RF}} = u_{\text{av}} \left[1 - \frac{1}{H} \int_0^H \left(1 - \frac{u^2(h)}{u_{\text{av}}^2} \right) \cos^2 \left(\frac{\pi p h}{H} \right) dh \right]^{1/2},$$

where $u_{\text{av}} \equiv (H^{-1} \int_0^H u^2(h) dh)^{1/2}$.

Our task here will be twofold: to compare the two preceding averages with each other, and to compare both of them with the standard spatial average

$$\langle u \rangle_{\text{SA}} = \frac{1}{H} \int_0^H u(h) dh,$$

which has already been used first by Ahlers^{5,6} and then by other authors.^{7,8} The more direct way to do that is to use as local velocity the isentropic velocity, for which its functional form (see below) is known. The integrals in h must be transformed, prior to their evaluation, into integrals in t . This is immediately done by using the relation (see Fig. 1) $t(h) = t^S + ah$, where $a \equiv -\rho g T'_\lambda$ and the superscript S stands for the top of the sample. In this way, for instance, the standard average becomes

$$\langle u \rangle_{\text{SA}}(t^S) = \frac{1}{aH} \int_{t^S}^{t^S + aH} u(t) dt. \quad (8)$$

The numerical results for the different averages and their t derivatives at various temperatures close to the λ line are displayed in Table II, for a sample depth of $H=2$ cm and SVP. The pertaining thermodynamic parameters

TABLE II. Different velocity averages and their t derivatives at various temperatures very near the λ line obtained using the isentropic velocity as local velocity: Flytime average (FT), resonant-frequency average (RF) for the two first plane-wave modes (noted by $p=1$ or 2), and standard spatial average (SA). See text for detailed definitions. Velocity values are in cm/s and t derivatives in cm/s μK .

t^S (μK)	-4	-1	0	1	4
$\langle u \rangle_{\text{FT}}$	21 761.37	21 765.23	21 773.30	21 778.83	21 784.86
$\langle u \rangle_{\text{RF}} (p=1)$	21 761.31	21 763.26	21 772.36	21 779.28	21 784.78
$\langle u \rangle_{\text{RF}} (p=2)$	21 761.46	21 765.62	21 772.61	21 778.51	21 784.95
$\langle u \rangle_{\text{SA}}$	21 761.37	21 765.24	21 773.31	21 778.83	21 784.86
$\frac{d\langle u \rangle_{\text{FT}}}{dt^S}$	-1.46	7.31	31.20	3.10	1.42
$\frac{d\langle u \rangle_{\text{RF}}}{dt^S} (p=1)$	-1.46	7.31	31.05	3.09	1.42
$\frac{d\langle u \rangle_{\text{RF}}}{dt^S} (p=2)$	-1.46	7.31	31.05	3.09	1.42
$\frac{d\langle u \rangle_{\text{SA}}}{dt^S}$	-1.46	7.31	31.10	3.09	1.42

for the isentropic velocity are from Ref. 17. We may see that the differences among the distinct averages and their temperature derivatives are less than 0.01% at any temperature. We have checked that this result is also valid at higher pressures. Due to the rounding of the velocity caused by dispersion, these differences will even decrease for real measurements ($\omega \neq 0$).

The conclusion from this comparison is that in the presence of inhomogeneity, the experimental velocity in the audio and ultrasonic frequency ranges is, independently of the experimental method used, very accurately represented by

$$\langle u \rangle_P(t^S, \omega) = \frac{1}{aH} \int_{t^S}^{t^S+aH} u_P(t, \omega) dt, \quad (9)$$

where we have rewritten Eq. (8) taking into account the local functional form obtained in Sec. II B.

For measurements in the hypersonic range ($\omega/2\pi \approx 1$ GHz), as for those carried out with light scattering techniques,^{10,19} it is precisely the presence of a very important velocity dispersion, as we shall see in Sec. IV, which guarantees the suppression of all measurable gravity effects. Note also that in this type of experiment performed in ⁴He liquid, the laser beam propagates horizontally. Other gravity corrections affecting directly such a propagation, as those analyzed by Canell²⁰ in other experiments, are also, with respect to first sound, negligible.

III. GRAVITY EFFECTS ON THE THERMODYNAMIC ($\omega=0$) VELOCITY

A. Local thermodynamic velocity

In this section we shall write the expressions for the local thermodynamic velocity in order to make the quantitative evaluations of the gravity effects formulated in Eq. (9). The study of this case ($\omega=0$) is interesting in that it is, as was argued above, the upper limit of the gravity effects in real ($\omega \neq 0$) measurements.

We begin with the basic expression for the isentropic first-sound velocity²¹

$$u^{-2} = \left[\frac{\partial P}{\partial \rho} \right]_S^{-1} = \rho K_S, \quad (10)$$

where $K_S = \rho^{-1}(\partial \rho / \partial P)_S$ is the isentropic compressibility. Next, we use the thermodynamic relations²¹

$$C_P - C_V = \frac{\alpha^2 VT}{K_T} \quad (11a)$$

and

$$\gamma = \frac{C_P}{C_V} = \frac{K_T}{K_S}, \quad (11b)$$

where $\alpha = -\rho^{-1}(\partial \rho / \partial T)_P$ is the thermal compressibility, C_P and C_V the specific heat at, respectively, constant pressure and volume, and V the specific volume.

Application of directional derivatives and the Maxwell relations yields

$$\alpha = \frac{1}{VT} T'_i C_P - \frac{1}{V} S'_i \quad (12a)$$

and

$$\kappa_T = \frac{C_P}{VT} T'_i - \frac{1}{V} S'_i T'_i - \frac{1}{V} V'_i, \quad (12b)$$

where we have used the notation $F'_i \equiv (\partial F / \partial P)_i$. Substitution of Eqs. (11) and (12) into Eq. (10) gives

$$u^{-2} = \frac{1}{V^2} \left[T'_i S'_i - V'_i - \frac{T}{C_P} (S'_i)^2 \right]. \quad (13)$$

When applied to $t=0$, we obtain

$$u_\lambda^{-2} = \frac{1}{V_\lambda^2} \left[T'_\lambda S'_\lambda - V'_\lambda - \frac{T_\lambda}{C_{P\lambda}} (S'_\lambda)^2 \right] \quad (14)$$

for the velocity at the λ line. The notation is $F_\lambda \equiv F(t=0)$ and $F'_\lambda \equiv (\partial F / \partial P)_{t=0}$. Equations (13) and (14) are exact, on the same basis of Eq. (10). Equation (13) for first sound is made more tractable upon the well-known cylindrical approximation,²² which can be stated as follows. Any magnitude can be expressed in the general form

$$F(P, t) = F_\lambda(P, t) + \Delta F(P, t).$$

The content of the cylindrical approximation is to assume that for the entropy and volume, ΔS and ΔV are independent of P . This amounts to admitting $S'_i = S'_\lambda$ and $V'_i = V'_\lambda$. With these assumptions along with the approximation $V = V_\lambda$, Eq. (13) results in

$$u(t) = \frac{T_\lambda (S'_\lambda)^2}{2V_\lambda^2} u_\lambda^3 \left[\frac{1}{C_P(t)} - \frac{1}{C_{P\lambda}} \right] + u_\lambda. \quad (15)$$

At this point, note the advantage of these manipulations: the only t -dependent magnitude is C_P , which is a very accurately measured quantity. However, there are two functional current representation for the specific heat at constant pressure:^{17,23,24} the power law C_P , for which $C_{P\lambda}$ is finite, and the logarithmic C_P representation, for which $C_{P\lambda}$ is infinite. In any case, from reference to thermodynamic data,¹⁷ we find $T/C_{P\lambda}, T'_\lambda S'_\lambda \ll -V'_\lambda$, which allows us to obtain the simple relation

$$u_\lambda = u_\lambda^0 + \frac{T_\lambda (S'_\lambda)^2}{2V_\lambda^2} (u_\lambda^0)^3 \frac{1}{C_{P\lambda}}, \quad (16)$$

where

$$u_\lambda^0 \equiv \frac{V_\lambda}{(T'_\lambda S'_\lambda - V'_\lambda)^{1/2}}. \quad (17)$$

Substitution of Eq. (16) into Eq. (15) gives

$$u(t) = A \frac{1}{C_P(t)} + u_\lambda^0, \quad (18)$$

with $A \equiv T_\lambda (S'_\lambda)^2 (u_\lambda^0)^3 / 2V_\lambda^2$ and u_λ^0 being only functions of pressure. The velocity u_λ^0 is consequently the velocity at $t=0$ if $1/C_{P\lambda}=0$, i.e., for the logarithmic C_P . The difference between the λ velocities for the power-law and logarithmic C_P , respectively, computed from Eq. (16) and using thermodynamic data¹⁷ is of the order of 20 cm/s, nearly independent of pressure. In order to obtain the pressure-dependent coefficients A and u_λ^0 , two methods

TABLE III. Values of first-sound velocity at the λ line assuming a logarithmic C_p and obtained from Eq. (17) using three difference thermodynamic data sources (noted I, II, and III), also directly from first-sound data.

P (bar)	u_λ (m/s)			Direct first-sound data ^d
	From Eq. (17) using different data sources	I ^a	II ^b	
0.06	217.1	217.4		217.3
5.01	253.9	254.7	241.0	255.6
9.21	278.1	278.7	269.5	279.6
15.24	304.6	305.0	293.6	307.0
20.4	321.5	322.0	313.0	325.4
25.46	335.2	334.3	328.3	339.9

^aReferences 17 and 27.

^bReference 26.

^cReference 23.

^dReference 8.

are available: from thermodynamic measurements and from the fit of Eq. (18) [or an extended version of it with an additional term linear in t valid for higher values of t (Ref. 25)] to first-sound velocity data at low frequency near the λ line. In this respect, we present in Table III a numerical comparison at different pressures for u_λ^0 obtained from thermodynamics according to Eq. (17) and from the fit to experimental velocity data. In the first three columns the values of V_λ and T'_λ [see Eq. (17)] are common and taken from Ref. 26. The two other magnitudes, namely S'_λ and V'_λ , are taken from the original measures of the corresponding authors, except for the data of Kierstead.²⁶ This last author did not measure S'_λ , so we have taken it from Ref. 17. However, we point out that the important parameter in u_λ^0 is V'_λ , $T'_\lambda S'_\lambda$ being about 40 times smaller. The velocity values of Carey *et al.*⁸ (fourth column) are normalized at $P=0.06$ bar to the value 218.08 m/s at $t=-40$ μ K, and in the corresponding fitting a logarithmic C_p with parameters of Ref. 17 has been used. Note firstly from Table III that among the values derived from thermodynamics, those of Okaji and Watanabe are discordant: we believe them to be somewhat undervalued. Secondly, the agreement between the values of Ahlers²⁷ or Kierstead²⁶ and those of Carey *et al.*⁸ at SVP worsen with increasing pressure. There is no explanation for this progressive discrepancy. It is of interest to point out that, although in any case the values in Table III are globally in agreement to within 4.5%, these differences can make up a much higher percentage (even more than 100%) when calculating, for example, the critical dispersion at $t=0$, where a precise background velocity must be known.

The functional form of the velocity in Eq. (18) is valid (its basis is the cylindrical approximation) in the temperature range⁹ $-t \lesssim 5 \times 10^{-3}$ K for He I and $t \lesssim 10^{-4}$ K for He II. We shall see later that gravity effects are well within these temperature ranges, so that Eq. (18) will suffice for all our purposes.

B. Average thermodynamic velocity ($\omega=0$) in a nonhomogeneous sample

We review here the influence of gravity on the isentropic velocity as detailed in Eq. (9). For C_p , we shall most-

ly adopt the simplified logarithmic expression $C_p = -A_0 \ln |t/T_\lambda| + B_0$, with coefficient values taken from Ref. 17 (nevertheless, the following results are independent of the detailed form adopted for C_p). The average velocity $\langle u \rangle$ can then be calculated straightforwardly according to Eq. (9). An example is shown in Fig. 2. The more relevant features of these calculations are as follows.

(i) The temperature at which the velocity is minimum is shifted by gravity from $t_{\min}=0$ to $t_{\min}^S = -(1-\delta)aH$. The correction δ depends on the two possible representations of C_p . This might, in principle, allow one to discriminate between the two representations, an important problem of critical behavior near T_λ still open.^{11,23,24} Unfortunately, we found the δ correction too small to induce observable effects: for the logarithmic C_p , $\delta=0.01$ and for the power-law C_p , $\delta=0.02$. Note also that, through a , t_{\min}^S has a weak pressure dependence, as can be seen in Fig. 2.

(ii) The difference between $\langle u \rangle$ and u is only appreci-

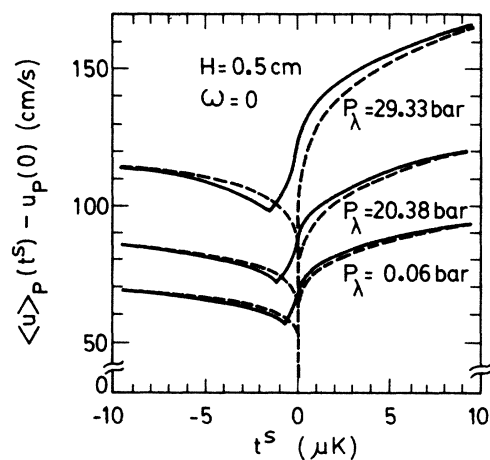


FIG. 2. Examples at various pressures of the gravity influence on the thermodynamic ($\omega=0$) first-sound velocity. The dashed curves are the gravity-free velocity differences $u_p(t,0) - u_p(0,0)$, and the solid curves are the corresponding gravity-affected velocity differences $\langle u \rangle_p(t,0) - u_p(0,0)$.

able in the range $|t^S| \lesssim 5 \mu\text{K}$, and has a sharp maximum at $t^S=0$. This difference, Δu , depends weakly on the sample depth and on the C_p representation. Thus for $H=0.5$ cm, $\Delta u_\lambda(t^S=0)$ ranges from 66 cm/s at SVP to 100 cm/s at the highest pressures, and for $H=2$ cm the variation over the same range of pressures is from 73 to 113 cm/s. These differences make up less than 0.4% of the total velocity, whatever the pressure or depth, but are nevertheless well within the precision of both velocity and temperature measurements. It must be also emphasized that they are of the same order of magnitude as the critical dispersion predicted by critical dynamic theories.⁹

It is worthwhile to remark that the above results cannot be *directly* tested. The reason is that within the temperature range of gravitational effects there is also, even for the lowest frequencies used (some few kHz), critical dispersion, an account of which will be made in the following. Certainly, low-frequency experimental velocity curves show a trend towards the above features, and this fact was actually a main motivation for the pioneering work of Ahlers on gravity effects.

IV. GRAVITY EFFECTS ON THE DISPERSIVE VELOCITY ($\omega \neq 0$)

A. Qualitative discussion

We analyze here to what extent the previous results on gravity effects are modified in real measurements, mainly due to the presence of dispersion. Unfortunately the influence of gravity in this case ($\omega \neq 0$) cannot be calculated by the same direct procedure as for $\omega=0$ because, due precisely to dispersion, the local velocity is now unknown. Therefore, we will proceed in the opposite way for $\omega=0$. In particular, instead of using Eq. (9), we start with the derivative version of it, i.e.,

$$\frac{d\langle u \rangle_P}{dt^S}(t^S, \omega) = \frac{1}{aH} [u_P(t^S + aH, \omega) - u_P(t^S, \omega)], \quad (19)$$

as a first step to relating the unknown local velocity $u_P(t, \omega)$ to the measured velocity $\langle u \rangle_P(t^S, \omega)$.

Before summarizing our numerical procedure, it is useful to make some geometric and intuitive considerations based on Eq. (19). Firstly, note that $d\langle u \rangle/dt^S$ is the slope that governs the variation in u over a temperature step of aH . In particular, the maximum fall in u for a temperature increment of aH occurs where this derivative is most negative, and it can be easily deduced from Eq. (19) that for $\omega=0$ this occurs at $t^S = -aH$, a typical value being -24 cm/s μK for $H=2$ cm and SVP. Surprisingly, graphical or numerical calculations of the minimum slopes $d\langle u \rangle/dt^S$ for any nonzero frequencies show them to be very much smaller in absolute magnitude than the corresponding zero-frequency slopes. For the SVP and $H=2$ cm case mentioned above, for instance, the value obtained using the data of Ref. 7 is -0.5 cm/s μK , and this difference by a factor of 50 between corresponding slopes is quite systematic. In other words, the u curves for even very low frequencies are some 50 times flatter than the corresponding zero-frequency u curves. The maximum difference between $\langle u \rangle$ and u should therefore

be reduced by approximately the same factor, which in view of the result for $\omega=0$ means that the maximum value of $\langle u \rangle - u$ should range from about 1 cm/s at SVP to about 2 cm/s at the highest pressures. Of course, this difference will fall even lower at higher frequencies.

The same kind of qualitative reasoning can be used to analyze the other main gravity effect, the temperature shift of the velocity minimum: All experimental $\langle u \rangle$ curves undergo a minimum near the λ line at $t^S < 0$, progressively less sharp as frequency increases. This means that $\langle u \rangle$ curves can be approximated, over a temperature interval of about aH (less than $15 \mu\text{K}$ except for atypical sample heights) around their minima by a parabolic profile, so much more accurately as frequency grows. Now then, if $\langle u \rangle$ is a parabole (it suffices to be over a t interval of aH around its minimum) and regardless of its opening, it is easily derived from Eq. (19) that u is also a parabole whose minimum is placed $aH/2$ temperature units to the right of that of $\langle u \rangle$, i.e., nearer the λ line. The partial conclusion is consequently that, whereas the gravity-induced temperature shift of the velocity minimum is aH K at $\omega=0$, this value should tend to $aH/2$ at higher frequencies.

B. Quantitative treatment

In order to obtain quantitatively u from $\langle u \rangle$, we have implemented a numerical procedure based on the following points. We have used polynomials of low degree (less than 5) to fit the experimental $\langle u \rangle$ curves over temperature intervals of about $3aH$. The resulting deviation is of the order of the experimental velocity resolution (~ 0.2 cm/s). From Eq. (19), as can be easily deduced, u will be another polynomial of the same degree, the coefficients of the u polynomial being simply and unambiguously related to those of the $\langle u \rangle$ polynomial. Let us illustrate these points with an example. Writing for $\langle u \rangle$ a polynomial of degree 5, for instance, in the form $\langle u \rangle = a_0 + a_1 t + a_2 t^2 + a_3 t^3 + a_4 t^4 + a_5 t^5$, we find that $u = b_0 + b_1 t + b_2 t^2 + b_3 t^3 + b_4 t^4 + b_5 t^5$, where

$$b_5 = a_5,$$

$$b_4 = a_4 - \frac{15}{6} a_5 (aH),$$

$$b_3 = a_3 - 2a_4 (aH) + \frac{5}{3} a_5 (aH)^2,$$

$$b_2 = a_2 - \frac{3}{2} a_3 (aH) + a_4 (aH)^2,$$

$$b_1 = a_1 - a_2 (aH) + \frac{1}{2} a_3 (aH)^2 - \frac{1}{6} a_5 (aH)^4,$$

and

$$b_0 = a_0 - \frac{1}{2} a_1 + \frac{1}{6} a_2 (aH)^2 - \frac{1}{30} a_4 (aH)^4$$

satisfies Eq. (19). *The difference in the values of both polynomials is a measure of the gravity effect in the concerned temperature region.* We proceed then in that way, covering successive temperature intervals until a systematic evaluation of the local velocity (affected by dispersion, but without rounding gravity) is achieved. The main quantitative results, obtained applying this method to the existing measurements, and which confirm the qualitative conclusions mentioned in Sec. IV A, are as follows: (i)

The difference between the temperatures at which the measured and local velocities are minima changes from almost aH at $\omega=0$ to $aH/2$ at a few tens of kHz, whatever the height of the sample and the pressure. (ii) Contrary to a common assumption,⁵⁻⁸ the difference between the measured and local velocities at $t^S=0$, which is of the order of 100 cm/s at $\omega=0$ for a sample of a few centimeters in height, drops sharply to below 10 cm/s in real measurements, even at frequencies of no more than a few kHz and whatever the (reasonable) depth of the sample or the pressure. An example of these temperature-shift and velocity-rounding features at $t^S=0$ is shown in Figs. 3(a) and 3(b), respectively, where the pronounced decrease of both effects as a function of frequency can be followed. The numerical results, noted by solid circles and triangles, have been processed from the data of Ref. 7. The solid lines are a guide for the eye. Both vertical axes are normalized to the corresponding thermodynamic limits (marked by arrows) with values $\Delta t_{\min}^S(0)=2.6 \mu\text{K}$ and $\Delta u_\lambda(0)=73 \text{ cm/s}$, computed according to Sec. IV and with the necessary parameters from Ref. 17. To further enlighten the finite-frequency influence on gravity effects, refer to Figs. 4(a) and 4(b). This figure shows a comparison between $\langle u \rangle - u$ at $\omega=0$ and $\omega/2\pi=6.6 \text{ kHz}$,

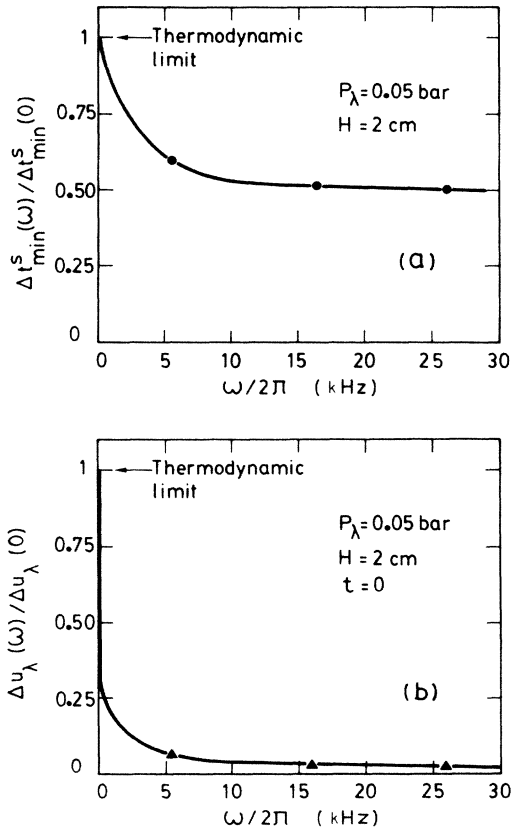


FIG. 3. A typical example showing the dramatic influence of dispersion on the gravity effects. (a) Temperature shift of the velocity minimum $\Delta t_{\min}^S \equiv t_{\min}^S(H) - t_{\min}^S(0)$. (b) Absolute value of the measured velocity minus the local thermodynamic velocity, both at T_λ : $\Delta u_\lambda \equiv \langle u \rangle_\lambda - u_\lambda$. Both curves in (a) and (b) are normalized to their corresponding thermodynamic ($\omega=0$) limit.

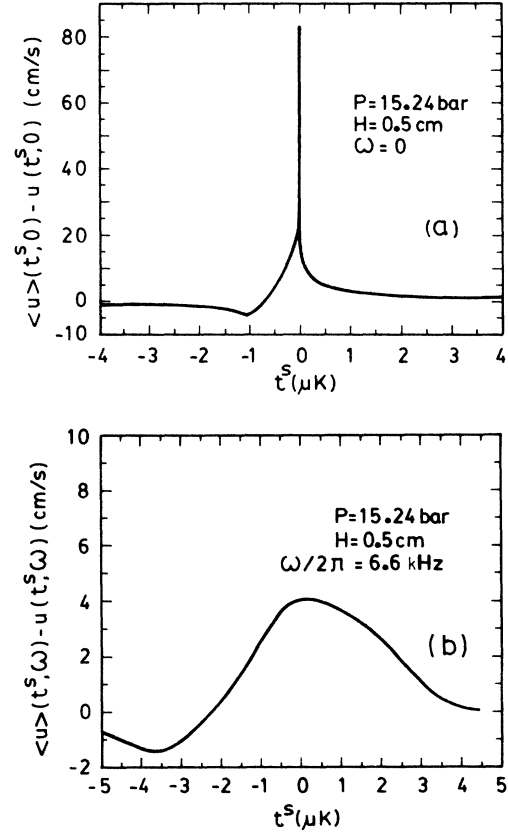


FIG. 4. Gravity effects on first-sound velocity as a function of the reduced temperature in a sample of 0.5 cm in height and at $P=15.24 \text{ bar}$. (a) In the thermodynamic limit ($\omega=0$). (b) In a real measurement, for a very low-frequency case (using a first resonant mode, $\omega/2\pi=6.6 \text{ kHz}$). This last curve is obtained by processing as indicated in the text, the data of Ref. 8. Note the different velocity scale in the two figures.

respectively, as a function of temperature. To obtain the curve in (b) following the procedure outlined above, the information from Ref. 8 was used.

V. CONCLUSIONS: AN ILLUSTRATIVE EXAMPLE

In this paper we have presented an analysis of the local and nonlocal gravity effects on the first-sound velocity near $T_\lambda(P)$ in liquid helium. Also, a numerical procedure to calculate quantitatively the gravity rounding effects on first-sound velocity in the presence of critical dispersion has been proposed. This method has been used to separate, for the first time, gravity and dispersion effects in real measurements. To illustrate the interest and capability of such a procedure, let us apply it to estimate the gravity corrections in one of the experimental situations mentioned in the Introduction of this paper: the comparison between the theoretical critical first-sound dispersion, $D(t, \omega)$, and the experiments. As a consequence of very basic assumptions,^{9,10} all the existing critical dynamic theories do not calculate the local velocity $u(t, \omega)$, but rather $D(t, \omega)$, defined by

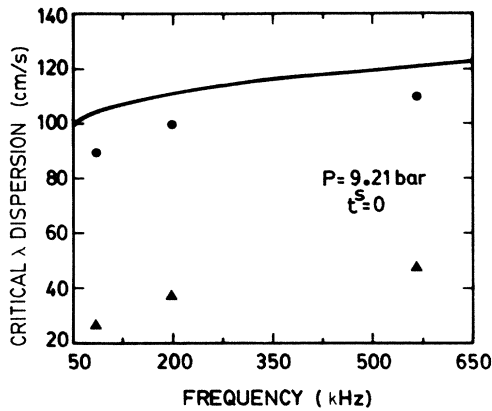


FIG. 5. A comparison between the two different treatments of the gravity effects on first-sound velocity measurements. Circles are the dispersion at T_λ obtained from the data of Ref. 8 by using the conventional treatment. Triangles are from the same data but processed following the procedure proposed in this paper. The solid line represents the dispersion predicted by dynamic scaling theories.

$$D(t, \omega) \equiv u(t, \omega) - u_B(T, 0),$$

where u_B is a local background or noncritical velocity. In contrast, from experiments one obtains

$$u_{\text{meas}} \equiv \langle u \rangle_M = \langle u(t, \omega) \rangle_M,$$

i.e., the absolute velocity affected by dispersion and also by the gravity inhomogeneity.

To obtain the experimental dispersion one must first estimate u_B . In general,^{8,10} u_B may easily be approximated by matching the functional form of the local (zero-frequency) velocity $u(t, 0)$ to the experimental $\langle u \rangle_M$ curves far away from T_λ , in a region where $\langle u \rangle_M$ is not affected by critical dispersion. The second step will be to introduce the gravity corrections. Until now,^{5,8} this was done by assuming that these corrections for $\langle u \rangle_M$ would be the same as for $u(t, 0)$, so that the "experimental" dispersion \tilde{D} to be compared with the theoretical one is

$$\tilde{D} \equiv \langle u(t, \omega) \rangle_M - \langle u(t, 0) \rangle. \quad (20)$$

An example of such a comparison is presented in Fig. 5. The solid line is $D(t, \omega)$ obtained from the dynamic scal-

ing theory of Ferrell and Bhattacharjee.^{9,28} The solid triangles are $\tilde{D}(t, \omega)$ obtained by applying Eq. (20) to the data of Ref. 8. The strong disagreement observed must not be a surprise for us, because we have clearly showed here that the two rounding mechanisms affecting $\langle u \rangle_M$, namely, the dispersion and the gravity inhomogeneity, are not linearly additives. If the procedure indicated in Sec. IV is used to find $u(t, \omega)$ from the experimental $\langle u(t, \omega) \rangle_M$ curves, and then one subtracts $u_B(t, 0)$ from these results, one finally obtains the solid circles, which are in much better agreement with the dynamic scaling results. A detailed account of these applications will be published elsewhere.²⁸

Note finally, that mainly due to the very accurate theoretical and experimental results available now, the rounding of the transition produced by nonintrinsic effects is one of the central problems encountered at the present time in the study of critical phenomena. As remarked in the Introduction, these rounding effects occur in all practical experiments and are produced by impurities, finite-sample effects, nonequilibrium behavior, or inhomogeneities. In general, it is very difficult to separate or to estimate the magnitude of these effects, mainly in the case of time-dependent or transport critical parameters, for which *intrinsic* rounding mechanisms may also be present. In fact, there exist very few quantitative studies of these nonintrinsic rounding effects in any system.¹ Therefore, the systematic results presented here for first sound near T_λ may provide some grounds to analyze other rounding effects in other transitions. In particular, the numerical procedure proposed here to separate the intrinsic (associated with dispersion) and the gravity rounding effects may easily be extended to analyze quantitatively sound-wave propagation near other second-order phase transitions.

ACKNOWLEDGMENTS

We are grateful to Professor F. Pobell for sending us the unpublished data corresponding to the experiments reported on in Refs. 7 and 8, and to Professor G. Ahlers, Professor V. Dohm, and Professor J. V. Sengers for making their results available to us before their publication. This work was supported in part by the Comisión Asesora de Investigación Científica y Técnica (CAICYT), Spain, under Grant No. 0620-84.

¹See, for instance, M. R. Moldover, J. V. Sengers, R. W. Gammon, and R. J. Hocken, *Rev. Mod. Phys.* **51**, 79 (1979).

²See, for instance, P. C. Hohenberg and M. Barmatz, *Phys. Rev. A* **6**, 289 (1972); M. Barmatz and P. C. Hohenberg, *Phys. Rev. Lett.* **24**, 1225 (1970).

³See, for instance, P. Pfeuty and G. Toulouse, *Introduction to the Renormalization Group and to Critical Phenomena* (Wiley, New York, 1977), Chap. 6.

⁴M. Barmatz and I. Rudnick, *Phys. Rev.* **170**, 224 (1968).

⁵G. Ahlers, *Phys. Rev.* **182**, 352 (1969).

⁶G. Ahlers, *J. Low Temp. Phys.* **1**, 609 (1969).

⁷W. C. Thomlison and F. Pobell, *Phys. Rev. Lett.* **5**, 283 (1973).

⁸R. Carey, C. H. Buchal, and F. Pobell, *Phys. Rev. B* **15**, 3133 (1977).

⁹R. A. Ferrell and J. K. Bhattacharjee, *Phys. Rev. Lett.* **44**, 403 (1980); *Phys. Rev. B* **23**, 2434 (1981); *ibid.* **28**, 121 (1983).

¹⁰F. Vidal, *Phys. Rev. B* **26**, 3986 (1982); *Phys. Lett. A* **92**, 89 (1982). References to high-frequency first-sound measurements are given here.

¹¹R. Dohm, *Z. Phys. B* **60**, 61 (1985); **61**, 193 (1985).

¹²G. Ahlers and P. C. Hohenberg, *Phys. Rev. Lett.* **52**, 313 (1984); R. A. Ferrell and J. K. Bhattacharjee, *ibid.* **52**, 314

- (1984); Phys. Rev. B 31, 1661 (1985).
- ¹³For a review of the highly active field of critical phenomena in microgravity conditions, and some of its applications to the λ line in ^4He , see, for instance, D. Beysens, in *Material Sciences in Space*, edited by B. Fenerbacher, H. Hamacher, and R. J. Nanman (Springer-Verlag, in press), Chap. 9.
- ¹⁴I. Rudnick, in *75th Jubilee Conference on Helium-4*, edited by J. G. M. Armitage (World Scientific, Singapore, 1983), p. 24.
- ¹⁵J. V. Sengers and J. M. J. van Leeuwen, Physica A 116, 245 (1982); J. Phys. Chem. (to be published).
- ¹⁶P. C. Hohenberg and B. I. Halperin, Rev. Mod. Phys. 49, 435 (1977).
- ¹⁷See, for instance, G. Ahlers, in *The Physics of Liquid and Solid Helium*, edited by K. H. Benneman and J. B. Ketterson (Wiley, New York, 1976), Chap. 2, Pt. I.; see also the tabulation data in C. P. Barenghi, P. Lucas, and R. J. Donnelly, J. Low Temp. Phys. 44, 491 (1981); R. P. Behringer and G. Ahlers, J. Fluid Mech. 125, 219 (1982), and references quoted therein.
- ¹⁸L. D. Landau and E. M. Lifshitz, *Statistical Physics* (Addison-Wesley, Reading, Mass., 1958), Sec. 111.
- ¹⁹F. Vidal, J. A. Tarvin, T. J. Greytak, Phys. Rev. B 25, 7040 (1982), and references therein.
- ²⁰D. S. Canell, Phys. Rev. A 16, 431 (1977), and references therein.
- ²¹See, for instance, S. Putterman, *Superfluid Hydrodynamics* (North-Holland, Amsterdam, 1974), Chap. I.
- ²²See, for example, M. J. Buckingham, and D. M. Fairbank, in *Progress in Low Temperature Physics*, edited by C. J. Gorter (North-Holland, Amsterdam, 1961), Vol. III, Chap. III.
- ²³M. Okaji and T. Watanabe, J. Low Temp. Phys. 32, 555 (1978); 49, 435 (1982).
- ²⁴J. A. Lipa, Physica B 107, 343 (1981).
- ²⁵R. A. Ferrell and J. K. Bhattacharjee, Phys. Rev. B 25, 3168 (1982).
- ²⁶H. A. Kierstead, Phys. Rev. 162, 153 (1967).
- ²⁷G. Ahlers, Phys. Rev. A 8, 530 (1973).
- ²⁸J. Maza and F. Vidal (unpublished).